RSC Advances

ROYAL SOCIETY OF CHEMISTRY

www.rsc.org/advances

HBT-based chemosensors for detection of fluoride through deprotonation process: experimental and DFT studies

Shudi Liu[a], Liangwei Zhang[a], Panpan Zhou[a], Wenyan Zan[a], Xiaojun Yao[a], Jingjun Yang[b], Ying Yang[a,b] *

E-mail address: yangying@lzu.edu.cn (Y. Yang)

Tel: 86-931-8912585; Fax: 86-931-8912582

[a] *Key Laboratory of Nonferrous Metals Chemistry and Resources Utilization of Gansu Province, College of Chemistry and Chemical Engineering, Lanzhou Univeristy, Lanzhou, 730000, PR China*

[b] *Gansu Normal University for Nationalities, Hezuo, 747000, PR China*

Abstract

In searching for developing fluoride chemosensors based on the O—H···F, we discovered that HBT-based fluorophore containing hydroxyl group was easily synthesized and displayed excellent fluorescence properties. 4-(benzothiazol-2-yl)-phenol (**L^{1}H**) was found to be facilitated in monitoring fluoride and shown ratiometric fluorescence changes. It was worth noting that an aldehyde group in conjugation with HBT-based fluorophore core at the adjacent position of hydroxyl group (5-(benzothiazol-2-yl)-2-hydroxylbenzaldehyde, **L^{2}H**) would elevate the sensitivity towards fluoride tremendously. Spectroscopic studies indicated that **L^{1}H** and **L^{2}H** interacted with fluoride anion and involved a two-step reaction: hydrogen bond formation and deprotonation. The deprotonation of the chemosensors by fluoride anion enhanced the electron-donating ability of phenolic O$^-$ to HBT core acceptor and facilitated the intramolecular charge transfer process resulting in the red-shift in both UV-*vis* absorption and fluorescence spectra. The mechanism of **L^{2}H** binding with fluoride was confirmed by ^{1}H NMR titration experiments and DFT computational calculations.

1. Introduction

Anions are widely present in natural environment and organisms since they play crucial roles in chemical and biological processes. As the smallest anion, fluoride has special physical and chemical properties. It plays vital roles in biological process as well as industry. In living organism, fluoride can be used in preventing odontopathy and osteoporosis.[1] In nuclear industry, as a consequence of the principle that fluoride could react with uranium, fluoride was used to separate radioactive and non-radioactive substances safely and easily[2]. However, excessive utilization of fluoride had inevitably leaded to severe environmental pollutions. Subsequently, fluoride accumulated in bodies by the food chains and eventually resulted in severe disease or death. Therefore, detections of fluoride have drawn great attentions.[3]

For the past few years, chemosensors for fluoride have been prosperously developed due to the properties of high sensitivity, excellent selectivity and low limit of detection. Many fluoride chemosensors were based on the interactions between fluoride and Lewis acids. A strategy for fluoride recognition was employing the formation of hydrogen bond. Fluoride can interact with thiourea,[4] urea,[5] amide,[6] sulfonamide,[7] imidazole,[8] indole,[9] pyrrole,[10] Schiff bases[11] and so on.[12] However, to the best of our knowledge, most of the recognition mechanisms mentioned above were based on the N—H···F but not O—H···F. Recently, the O—H···F was considered as of great concern.[13] Cao group designed new fluoride sensors that taken into the reason that O—H has higher electronegativity and acidity than N—H.[13b] However, both the receptors undergone an "OFF-ON-OFF" process, viz., that the fluorescence intensity would be quenched when the amount of F⁻ reached up to more than 6 equiv. and this self-quenching caused by concentration would disturb the detection results and greatly limited its application. As our ongoing interest to develop fluorescent probes for fluoride based on the O—H···F, we recently endeavored to explore kinds of fluorophores containing hydroxyl group. We discovered that HBT-based fluorophore was easily synthesized, cheaply consumed and displayed excellent fluorescence properties. As expected, the compound, 4-(benzothiazol-2-yl)-phenol (**L¹H**) containing hydroxyl group was found to be facilitated in monitoring fluoride and shown ratiometric fluorescence changes. Although **L¹H** displayed high sensitivity toward fluoride, it needed to add amounts of F⁻ (less than 10 equiv.)

3

until the fluorescence reach up to saturated state. It was worth noting that an aldehyde group in conjugation with HBT-based fluorophore core at the adjacent position of hydroxyl group (5-(benzothiazol-2-yl)-2-hydroxylbenzaldehyde, $\mathbf{L^2H}$) would elevate the sensitivity towards fluoride tremendously. The interaction between $\mathbf{L^2H}$ and fluoride may involve a two-step reaction: hydrogen bond formation and deprotonation, and the structures and proposed binding mechanisms were shown in Scheme 1. Mechanistic studies were confirmed by spectroscopic studies, ^{1}H NMR titration experiments and DFT computational calculations.
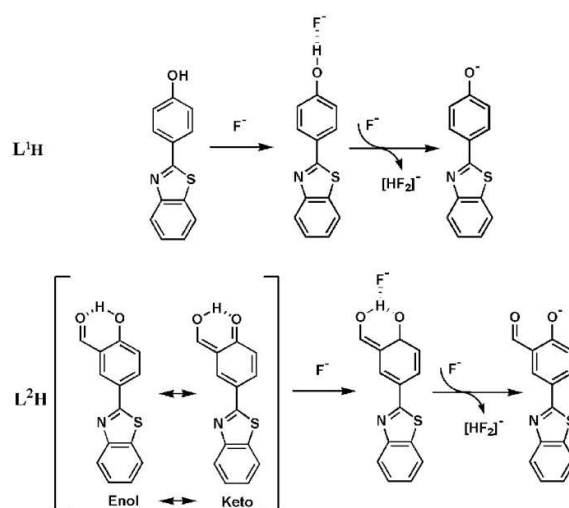
Scheme 1 Structures and proposed binding mechanisms of $\mathbf{L^1H}$ and $\mathbf{L^2H}$ with F⁻.

2. Experimental

2.1 Materials and instruments

All starting materials and reagents (analytical grade) concluding the tetrabutylammonium salts of halides and sodium salts of other anions were supplied by commercial suppliers and used without further purification. THF was used as HPLC grade. ^{1}H NMR titration experiments were recorded on a JNM_ECS 400 instruments. Fluorescence spectra were successively achieved by a Thermo Scientific Lumina fluorescence spectrometer. UV-*vis* absorption spectra were accomplished on an Evolution 220 UV-Visible spectrometer. Fluorescence quantum yield were performed by absolute value method on a FL sp920.

2.2 Synthesis and characterization of L^1H and L^2H

The synthetic methods of L^1H and L^2H were mentioned in our previous literatures.[14]

2.3 Absorption and fluorescence preparation

The stock solutions of L^1H and L^2H (1 mM) were prepared in THF while anions (10 mM) were prepared in triple deionized water. The solutions of anions (1 mM) were diluted by putting the concentrated 10 mM solutions into THF. All of the absorption and fluorescence measurements were implemented in a quartz cell (1 cm×1 cm×3.5 cm). UV-*vis* absorption titrations and fluorescence titrations were performed by adding F^- into 2 ml THF with L^1H or L^2H in advance diluted in it. The fluorescent spectra were carried out by excitation at 330 nm. Both the slit widths in excitation and emission were 5 nm. The detection limit was calculated as the ratio of $3\sigma/k$.[14b, 15] σ stands for the standard deviation of 10 times measurement of the emission spectrum of L^2H, k is the slope by plotting the fluorescence intensity of L^1H or L^2H upon addition of various amount of F^-. The dissociation constant K_d was fitted by the equation that $K_d = [X]^n \cdot (F_{max}-F) / (F-F_{min})$. F_{min}, F_{max} and F present the emission intensities in the absence of fluoride, presence of fluoride in saturation and any contents of fluoride in varying, [X] is the concentration of fluoride, n is the number of fluoride bound per L^1H or L^2H.

2.4 DFT computational studies

The optimized geometries for the structures in Scheme 1 were obtained by employing quantum mechanical calculations which were carried out at the B3LYP/6-311+G(d,p) level of theory using the Gaussian 09 suite of programs.[16] The IEFPCM solvation model was used for the calculations and THF was used as the solvent which was in agreement with the experiment condition.

3. Results and discussion

3.1 The UV-*vis* absorption and fluorescence spectrum studies of L^1H

In order to search for new fluoride chemsensors, we using $\mathbf{L^1H}$ （HBT-based compound containing hydroxyl group）as a novel prototype. It was found to be facilitated in monitoring fluoride anion by UV-*vis* absorption and fluorescence emission spectra. In Fig. 1a, $\mathbf{L^1H}$ has an absorption peak at 320 nm and a shoulder peak at 309 nm in THF. While fluoride was added from 0 to 95 μM, the peak at 309 nm and 320nm decreased gradually and a new peak at 376 nm appeared and increased simultaneously with an isobestic point at 330 nm. The changes in absorbance at 320 nm and 376 nm were presented in Fig. 1a (Inset), respectively. In the meantime, the emission peak of $\mathbf{L^1H}$ at 368 nm is decreased gradually and a new peak at 426 nm increased simultaneously in fluorescence spectra of $\mathbf{L^1H}$ (Fig. 1b). The detection limit of $\mathbf{L^1H}$ was calculated to be 6.70×10^{-8} M by fluorescence titration and the dissociation constant was obtained to be 8.28×10^{-10} M^2 as well (Fig. S1 and Fig. S2). In terms of sensitivity for fluoride, $\mathbf{L^1H}$ is superior to previous probes.[13] However, $\mathbf{L^1H}$ need more fluoride to achieve equilibration which inevitably leaded to weak sensitivity. Hence, it is necessary to explore the method that through modifying the structure of $\mathbf{L^1H}$ to improve the sensing ability.
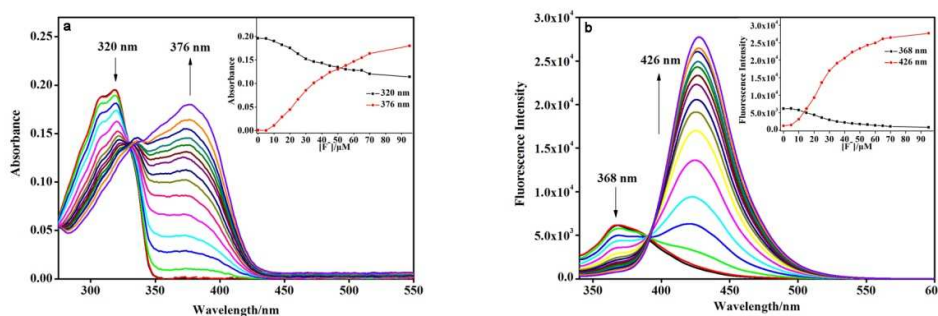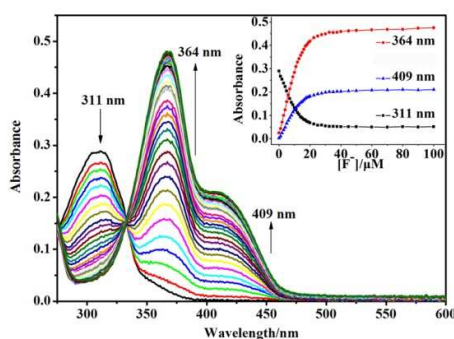

Fig. 1 UV-*vis* absorption spectra (a) and fluorescence emission spectra (b) of $\mathbf{L^1H}$ (10 μM) upon addition of various amount of F⁻ (0 – 95 μM) in THF. Inset: (a) Changes in absorbance at 320 nm and 376 nm, respectively; (b) Changes in fluorescence intensity at 368 nm and 426 nm, respectively.

3.2 UV-*vis* absorption and fluorescence spectrum studies of $\mathbf{L^2H}$

To greatly improve the properties, $\mathbf{L^2H}$ was obtained by conjugation an aldehyde group to HBT-based fluorophore core at the adjacent position of hydroxyl group. Remarkably, the sensitivity and the detection limit of $\mathbf{L^2H}$ towards fluoride anion were elevated after the

modification. As depicted in Fig. 2, UV-*vis* absorption titrations were implemented in THF at room temperature. There was only an absorption band at 311 nm in the condition of 2 ml THF containing 10 μM of **L²H**. Upon addition of fluoride from 0 to 100 μM, the absorption band at 311 nm was gradually decreased while two new bands at 364 nm and 409 nm were continuously increased and companied with an isobestic point at 330 nm. The two new peaks were simultaneously formed mainly caused by the reason that deprotonation form of **L²H** existed two tautomeric forms (*Enol* and *Keto*) after **L²H** interacted with fluoride anion. The absorbance changes at 311 nm, 364 nm and 409 nm were shown respectively in Fig. 2, Inset. The absorbance was remained unchanged since the content of fluoride reached up to 20 μM implied that **L²H** could react with 2 equiv. of fluoride.

**Fig. 2** UV-*vis* absorption spectra of **L²H** (10 μM) upon addition of various amount of F⁻ (0 – 100 μM) in THF. Inset: Changes in absorbance at 311 nm, 364 nm and 409 nm, respectively.

Using the isobestic point at 330 nm as the excitation, fluorescence titration spectra of **L²H** versus various amount of fluoride were exhibited in Fig. 3. Along with the addition of fluoride, the fluorescence intensity at 480 nm increased remarkably and ultimately saturated if fluoride added up to 2 equiv. of **L²H**. The ratio of fluorescent intensity at 480 nm could reach up to 102 fold in THF in case that **L²H** /F⁻ was 1:2 (Fig. 3, Inset). The fluorescence quantum yield (Φ) of **L²H** was 20.56%, while Φ of **L²H** in addition with 2 equiv. of F⁻ was 52.23%. To further identify the ratio of **L²H** and fluoride as we predicted in Scheme 1, Job's plot was experimented in the condition that different amounts of **L²H** were in addition with relevant different levels of F⁻ in THF at 480

nm. The total content of L^2H and F^- was 10 μM. As was illustrated in Fig. 4, L^2H could react with 2 equiv. of fluoride. The detection limit of L^2H was calculated to be 4.23×10^{-8} M by fluorescence titration and the dissociation constant of L^2H was counted to be 7.07×10^{-11} M^2 as well (Fig. S3 and Fig. S4). The existence of aldehyde group elevated the properties of L^2H towards fluoride anion, due to the aldehyde group could form hydrogen bond with hydroxyl group of HBT core which weakening the interaction between oxygen and hydrogen of hydroxyl group. The hydrogen atom would lose more easily. Focusing on the selectivity of L^2H, many anions were participated in comparison. In Fig. 5, upon treatment of L^2H with fluoride anion, dramatic fluorescence intensity increasement was observed. In contrast, only addition of I^-, Ac^- and PO_4^{3-} lead to slight fluorescence changes of L^2H, the other representative anions did not cause any significant fluorescence response. What's more, the fluorescence intensity upon the subsequent addition of fluoride presented inordinate increasement. The ratiometric changes and bathochromic shift of L^1H and L^2H after binding with fluoride probably originated from the process of hydrogen bond formation and deprotonation, which was attributed to the basicity and strong ability of fluoride anion to from hydrogen bond and the stabilized $[HF_2]^-$.[3d, 10a] The occurrence of the process further enhanced the electron-donating ability of phenolic O^- to HBT core acceptor resulting in the intramolecular charge transfer process. To confirm the process, L^2H binding with fluoride was confirmed by ^{1}H NMR titration experiments and DFT computational calculations.
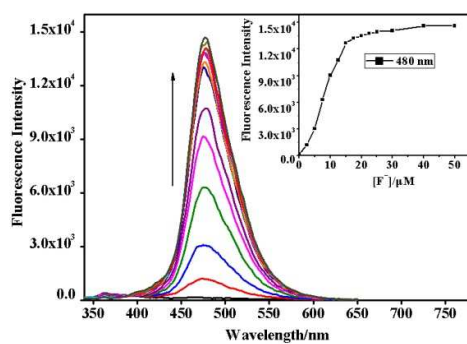
Fig. 3 Fluorescence emission spectra of L^2H (10 μM) upon addition of various amount of F^- (0 – 50 μM) in THF. Excitation was at 330 nm. Inset: Changes of fluorescence intensity at 480 nm.

8
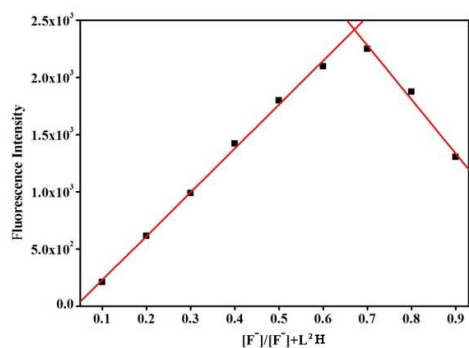
Fig. 4 Job's plot of different amount of L^2H in addition with relevant different levels of F^- in THF at 480 nm. The total content of L^2H and F^- was 10 μM.
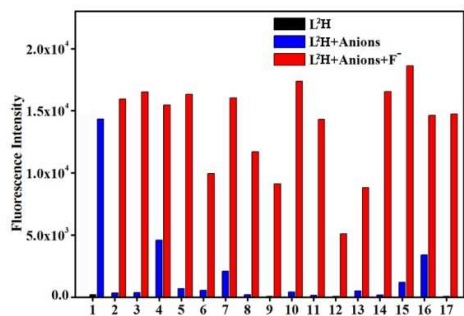

Fig. 5 Fluorescent intensity changes of L^2H (10 μM) upon addition of various different anions. The black bar represents the fluorescence intensity of L^2H; the blue bars represent the fluorescence intensities of L^2H response to different anions (50 μM): (1)F^-, (2) Cl^-, (3) Br^-, (4) I^-, (5) S^{2-}, (6) HS^-, (7) PO_4^{3-}, (8) BrO_3^-, (9) $H_2PO_4^-$, (10) HCO_3^-, (11) SO_3^{2-}, (12) HSO_4^-, (13) $S_2O_3^{2-}$, (14) HPO_4^{2-}, (15) CO_3^{2-}, (16) Ac^- and (17) HSO_3^-; the red bars represents the fluorescence intensity that occur upon the subsequent addition of 50 μM F^- to above solution.

### 3.3 Studies on the mechanism of L^2H versus fluoride

In order to validate the proposed process, ^1H NMR titrations were performed in $CDCl_3$-THF mixed solvent. As shown in Fig. 6, significant spectral changes were observed with gradual addition of certain concentrations of F^-. It was noticeable that the phenol OH proton signal (10.70

ppm) was disappeared as soon as fluoride anion was added to the mixed solution of **L²H**. As increasing concentrations of fluoride, the signals of H (2, 3, 4, 5, 6, 7) protons were gradually shift upfield while the other H (1, 8) protons were shift downfield. Also the signal of $[HF_2]^-$ was observed at low field and shown in Fig. S5. However, the signals of protons were very weak when the amount of fluoride reached up to 1.5 equiv., so the titration experiments was not completed as the initial scheme designed to reach 2 equiv.. Even so, the results suggesting that the interaction between **L²H** and fluoride anion undergo a two-step reaction: hydrogen bond formation and deprotonation. The final deprotonation of **L²H** by fluoride anion enhanced the electron-donating ability of phenolic O^- to HBT core acceptor and facilitated the intramolecular charge transfer process.
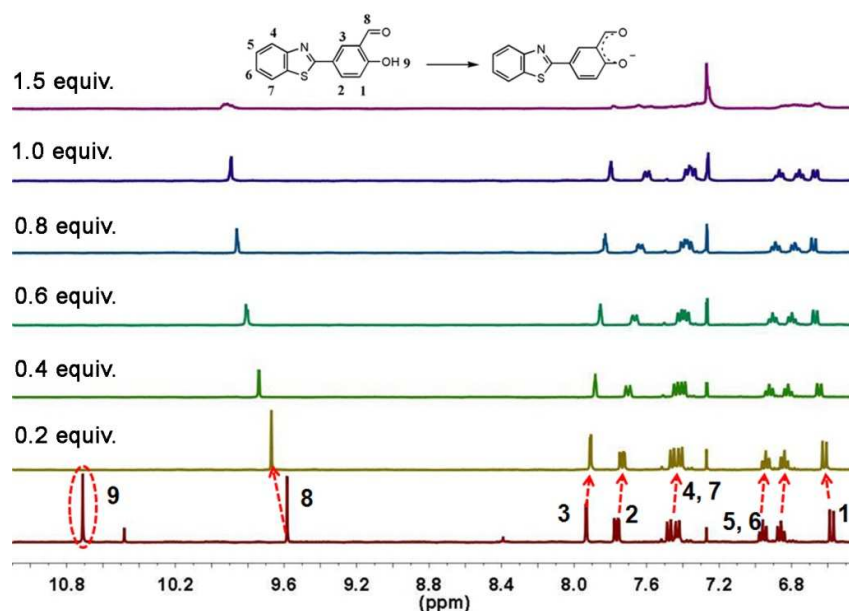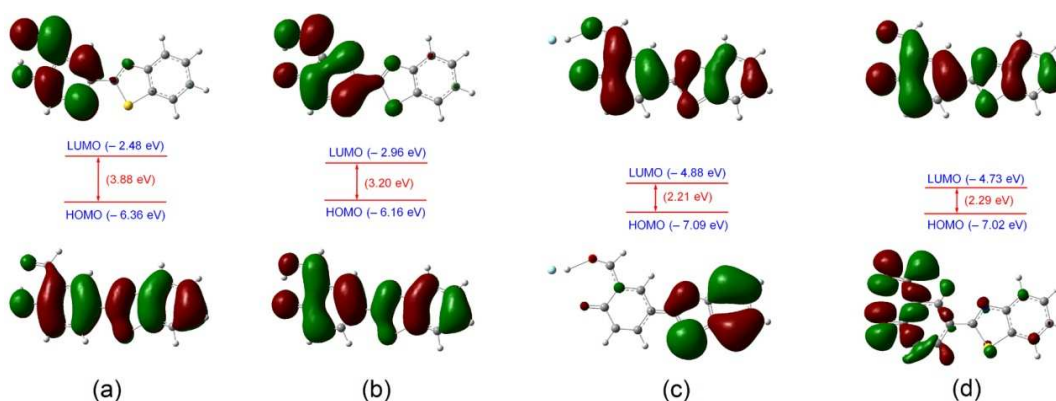

Fig. 6 Partial ¹H NMR spectra of probe **L²H** in the presence of a different amount of F⁻ in CDCl₃-THF (V/V, 2/3) mixed solvent.

3.4 DFT computational studies
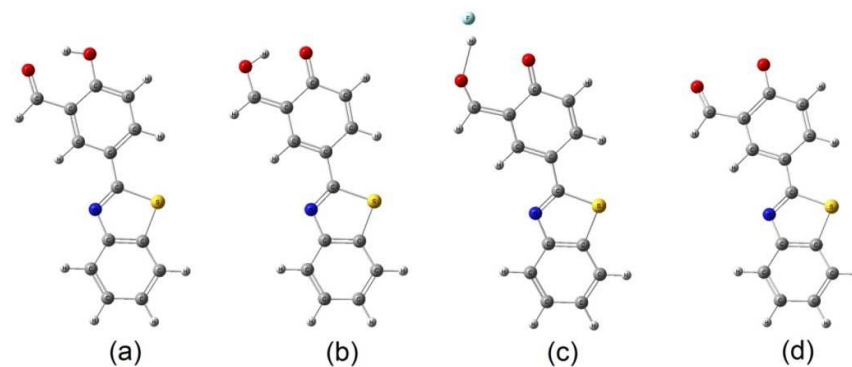
Fig. 7 Optimized geometry structures of **L²H** (*Enol*, a), **L²H** (*Keto*, b), **L²H** -F⁻ (c) and (**L²**)⁻ (d).

Fig. 8 Frontier molecular orbitals (HOMO, LUMO) for (a) **L²H** (*Enol*); (b) **L²H** (*Keto*); (c) **L²H** -F⁻; and (d) (**L²**)⁻, and the HOMO-LUMO energy gaps obtained by DFT calculation.

To better understand the spectral behaviors of **L²H** before and after binding with F⁻, theoretical calculations were performed. The results of these calculations were shown in Fig. 7 and Fig. 8. **L²H** intrinsically displayed two fluorescence emission peaks at 355 nm and 460 nm (Fig. S6), which was due to **L²H** in presence in of tautomeric forms, *Enol* and *Keto*. After binding with F⁻, the O—H⋯F hydrogen bond was formed which was resulted from the weak interaction between hydrogen and fluoride. The optimized geometry structures of four forms were shown in Fig.7. In Fig.8, in the process of **L²H** interact with fluoride, both the molecular orbital diagrams of HOMOs and LUMOs are redistributed in four forms. The energy gap between the HOMOs and LUMOs in four forms is become smaller after interacted with fluoride. The changes are in good agreement with the red shift in the absorption observed upon treatment of **L²H** with fluoride.

4. Conclusions

In conclusion, we had developed two HBT-based chemosensors (**L¹H**, **L²H**) containing hydroxyl group for detection of fluoride anion. Spectroscopic studies indicated that an aldehyde group in conjugation with **L¹H** core at the adjacent position of hydroxyl group would elevate the sensitivity towards fluoride tremendously. The studies suggested that the process of **L¹H** and **L²H** sensing fluoride anion involved a two-step reaction: hydrogen bond formation and deprotonation. The final deprotonation of the chemosensors by fluoride anion enhanced the electron-donating ability of phenolic O⁻ to HBT core acceptor and facilitated the intramolecular charge transfer process resulting in the red-shift in both UV-*vis* absorption and fluorescence spectra. The mechanism of **L²H** binding with fluoride was confirmed by ¹H NMR titration experiments and DFT computational calculations.
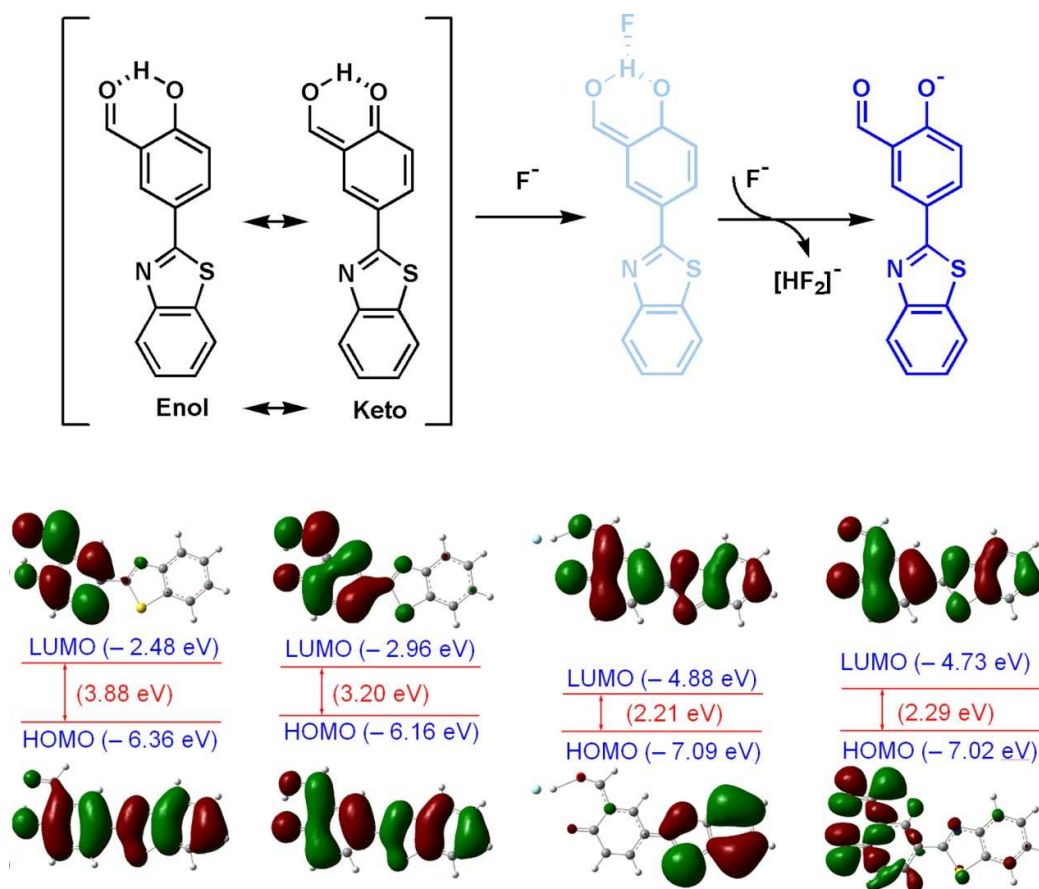
Acknowledgements

References

[1] M. Kleerekoper, *Endocrinol. Metab. Clin. North. Am.* **1998**, *27*, 441-452.

[2] a) M. Gavrilescu, L. V. Pavel and I. Cretescu, *J. Hazard. Mater.* **2009**, *163*, 475-510; b) G. H. John, I. May, D. Collison and M. Helliwell, *Polyhedron.* **2004**, *23*, 3097-3103; c) J. Seneda, F. Figueiredo, A. Abrao, F. Carvalho and E. Frajndlich, *J. Alloys Compd.* **2001**, *323*, 838-841.

[3] a) Y. Zhou, J. F. Zhang and J. Yoon, *Chem. Rev.* **2014**, *114*, 5511-5571; b) L. S. Natrajan, *Coord. Chem. Rev.* **2012**, *256*, 1583-1603; c) K. Kikuchi, *Chem. Soc. Rev.* **2010**, *39*, 2048-2053; d) T. Gunnlaugsson, M. Glynn, G. M. Tocci, P. E. Kruger and F. M. Pfeffer, *Coord. Chem. Rev.* **2006**, *250*, 3094-3117.

[4] a) E. J. Jun, K. M. K. Swamy, H. Bang, S. J. Kim and J. Yoon, *Tetrahedron Lett.* **2006**, *47*, 3103-3106; b) S. Devaraj, D. Saravanakumar and M. Kandaswamy, *Sens. Actuators, B* **2009**, *136*, 13-19; c) M. Vazquez, L. Fabbrizzi, A. Taglietti, R. M. Pedrido, A. M. Gonzalez-Noya and M. R. Bermejo, *Angew. Chem. Int. Ed.* **2004**, *43*, 1962-1965; d) W. Lu, M. Zhang, K. Liu, B. Fan, Z. Xia and L. Jiang, *Sens. Actuators, B* **2011**, *160*, 1005-1010; e) V. Thiagarajan, P. Ramamurthy, D. Thirumalai and V. T. Ramakrishnan, *Org. Lett.* **2005**, *7*, 657-660; f) L. E. Santos-Figueroa, M. E. Moragues, M. M. Raposo, R. M. Batista, S. P. Costa, R. C. Ferreira, F. Sancenon, R. Martinez-Manez, J. V. Ros-Lis and J. Soto, *Org. Biomol. Chem.* **2012**, *10*, 7418-7428.

[5] a) M. Boiocchi, L. Del Boca, D. E. Gomez, L. Fabbrizzi, M. Licchelli and E. Monzani, *J. Am. Chem. Soc.* **2004**, *126*, 16507-16514; b) S. K. Kim and J. Yoon, *Chem. Commun.* **2002**, 770-771; c) E. J. Cho, J. W. Moon, S. W. Ko, J. Y. Lee, S. K. Kim, J. Yoon and K. C. Nam, *J. Am. Chem. Soc.* **2003**, *125*, 12376-12377; d) Y. Wu, X. Peng, J. Fan, S. Gao, M. Tian, J. Zhao and S. Sun, *J. Org. Chem.* **2007**, *72*, 62-70.

[6] a) S. Wang, W. Shen, Y. Feng and H. Tian, *Chem. Commun.* **2006**, 1497-1499; b) Y. Li, L. Cao and H. Tian, *The J. Org. Chem.* **2006**, *71*, 8279-8282; c) B. Ke, W. Chen, N. Ni, Y. Cheng, C. Dai, H. Dinh and B. Wang, *Chem. Commun.* **2013**, *49*, 2494-2496; d) B. Liu and H. Tian, *J. Mater. Chem.* **2005**, *15*, 2681-2686; e) H. C. Hung, Y. Y. Chang, L. Luo, C. H. Hung, E. W. Diau and W. S. Chung, *Photochem. Photobiol. Sci.* **2014**, *13*, 370-379.

[7] a) S. V. Bhosale, S. V. Bhosale, M. B. Kalyankar and S. J. Langford, *Org. Lett.* **2009**, *11*, 5418-5421; b) H. Lu, W. Xu, D. Zhang, C. Chen and D. Zhu, *Org. Lett.* **2005**, *7*, 4629-4632; c) H. G. Im, H. Y. Kim, M. G. Choi and S. K. Chang, *Org. Biomol. Chem.* **2013**, *11*, 2966-2971; d) L. Fu, F. F. Tian, L. Lai, Y. Liu, P. D. Harvey and F. L. Jiang, *Sens. Actuators, B* **2014**, *193*, 701-707.

[8] a) H. N. Lee, N. J. Singh, S. K. Kim, J. Y. Kwon, Y. Y. Kim, K. S. Kim and J. Yoon, *Tetrahedron Lett.* **2007**, *48*, 169-172; b) J. Yoon, S. K. Kim, N. J. Singh and K. S. Kim, *Chem. Soc. Rev.* **2006**, *35*, 355-360.

[9] a) X. He, S. Hu, K. Liu, Y. Guo, J. Xu and S. Shao, *Org. Lett.* **2006**, *8*, 333-336; b) G. Pereira, E. M. S. Castanheira, P. M. T. Ferreira and M. J. R. P. Queiroz, *Eur. J. Org. Chem.* **2010**, *2010*, 464-475.

[10] a) A. K. Mahapatra, R. Maji, K. Maiti, S. S. Adhikari, C. Das Mukhopadhyay and D. Mandal, *Analyst* **2014**, *139*, 309-317; b) S. Rivadehi, E. F. Reid, C. F. Hogan, S. V. Bhosale and S. J. Langford, *Org. Biomol. Chem.* **2012**, *10*, 705-709.

[11] a) K. Liu, X. Zhao, Q. Liu, J. Huo, H. Fu and Y. Wang, *J. Photochem. Photobiol. B* **2014**, *138*, 75-79; b) K. K. Upadhyay, R. K. Mishra, V. Kumar and P. K. R. Chowdhury, *Talanta.* **2010**, *82*, 312-318; c) X. Bao, J. Yu and Y. Zhou, *Sens. Actuators, B* **2009**, *140*, 467-472.

[12] a) A. B. Sariguney, A. O. Saf and A. Coskun, *Spectrochim. Acta A Mol. Biomol. Spectrosc.* **2014**, *128*, 575-582; b) B. Sui, B. Kim, Y. Zhang, A. Frazer and K. D. Belfield, *ACS Appl. Mater. Interfaces* **2013**, *5*, 2920-2923; c) P. Zhao, J. Jiang, B. Leng and H. Tian, *Macromol. Rapid. Commun.* **2009**, *30*, 1715-1718; d) J. S. Chen, P. W. Zhou, G. Y. Li, T. S. Chu and G. Z. He, *J. Phys. Chem. B* **2013**, *117*, 5212-5221; e) J. S. Chen, P. W. Zhou, S. Q. Yang, A. P. Fu and T. S. Chu, *Phys. Chem. Chem. Phys.* **2013**, *15*, 16183-16189; f) J. S. Chen, R. Z. Liu, Y. Yang and T. S. Chu, *Theor. Chem. Acc.* **2013**, *133*; g) J. S. Chen, P. W. Zhou, L. Zhao and T. S. Chu, *RSC Adv.* **2014**, *4*, 254.

[13] a) J. T. Ma, Z. Li, Y. Q. Zong, Y. Men and G. W. Xing, *Tetrahedron Lett.* **2013**, *54*, 1348-1351; b) Q. Y. Cao, M. Li, L. Zhou and Z. W. Wang, *RSC Adv.* **2014**, *4*, 4041-4046; c) A. K. Mahapatra, K. Maiti, P. Sahoo and P. K. Nandi, *J. Lumin.* **2013**, *143*, 349-354.

[14] a) S. D. Liu, L. W. Zhang and X. Liu, *New J. Chem.* **2013**, *37*, 821-826; b) S. Liu, L. Zhang, W. Zan, X. Yao, Y. Yang and X. Liu, *Sens. Actuators, B* **2014**, *192*, 386-392.

[15] a) L. Zhang, X. Cui, J. Sun, Y. Wang, W. Li and J. Fang, *Bioorg. Med. Chem. Lett.* **2013**, *23*, 3511-3514; b) L. Zhang, D. Duan, X. Cui, J. Sun and J. Fang, *Tetrahedron* **2013**, *69*, 15-21.

[16] M. J. Frisch, G. W. Trucks, H. B. Schlegel, G. E. Scuseria, M. A. Robb, J. R. Cheeseman, G. Scalmani, V. Barone, B. Mennucci, G. A. Petersson, H. Nakatsuji, M. Caricato, X. Li, H. P. Hratchian, A. F. Izmaylov, J. Bloino, G. Zheng, J. L. Sonnenberg, M. Hada, M. Ehara, K. Toyota, R. Fukuda, J. Hasegawa, M. Ishida, T. Nakajima, Y. Honda, O. Kitao, H. Nakai, T. Vreven, J. A. Montgomery, Jr., J. E. Peralta, F. Ogliaro, M. Bearpark, J. J. Heyd, E. Brothers, K. Kudin, N., V. N. Staroverov, R. Kobayashi, J. Normand, K. Raghavachari, A. Rendell, J. C. Burant, S. S. Iyengar, J. Tomasi, M. Cossi, N. Rega, N. J. Millam, M. Klene, J. E. Knox, J. B. Cross, V. Bakken, C. Adamo, J. Jaramillo, R. Gomperts, R. E. Stratmann, O. Yazyev, A. J. Austin, R.

Cammi, C. Pomelli, J. W. Ochterski, R. L. Martin, K. Morokuma, V. G. Zakrzewski, G. A. Voth, P. Salvador, J. J. Dannenberg, S. Dapprich, A. D. Daniels, O. Farkas, J. B. Foresman, J. V. Ortiz, J. Cioslowski and D. J. Fox in *Gaussian 09, Revision, C. 01*, *Vol.* Gaussian, Inc., Wallingford CT, **2009**.

Graphical abstract